# Stereochemistry Driven Distribution of 1,4-Diaminocyclohexane Residues over the Crystalline and Amorphous Phase in Copolyamides 4.14/1,4-DACH.14. A Solid-State NMR and Temperature-Dependent WAXD Study

**Bert Vanhaecht,[†] Bart Goderis,[‡] Pieter C. M. M. Magusin,[§] Brahim Mezari,[§] Igor Dolbnya,[⊥] and Cor E. Koning*[,†,#]**

*Department of Physical and Colloidal Chemistry, Free University of Brussels (VUB), Pleinlaan 2, 1050 Brussels, Belgium; Chemistry Department, Catholic University of Leuven, Celestijnenlaan 200F, B-3001 Heverlee, Belgium; Laboratory of Inorganic Chemistry and Catalysis, Eindhoven University of Technology, P.O. Box 513, 5600MB Eindhoven, The Netherlands; DUBBLE-CRG/ESRF, Rue des Martyrs 156, B.P. 220, F-38043 Grenoble Cedex, France; and Laboratory of Polymer Chemistry, Eindhoven University of Technology, P.O. Box 513, 5600MB Eindhoven, The Netherlands*

*Received January 12, 2005; Revised Manuscript Received May 9, 2005*

ABSTRACT: Following our previous study on the stereoselective cocrystallization of linear and cyclic dicarboxylic acid residues in copolyamides 12.6/12.1,4-cyclohexanedicarboxylic acid (12.6/12.1,4-CHDA, Vanhaecht et al., *Macromolecules* **2004**, *37*, 421), we have now investigated a series of copolyamides containing trans or cis isomers of 1,4-diaminocyclohexane (1,4-DACH), viz. 4.14/1,4-DACH.14. Solid-state NMR studies and WAXD experiments demonstrate that the cis isomer is present in the amorphous regions of the copolyamide, whereas the trans isomer is located in both the crystalline and the amorphous phase. Similar to the results for the *trans*-1,4-CHDA-based copolyamides, *trans*-1,4-DACH moieties are probably built into the crystalline structure with the cycloaliphatic ring oriented perpendicular to the hydrogen-bonded crystal sheets. Temperature-dependent WAXD patterns show that, unlike in the homopolyamide 4.14, a pseudohexagonal phase is not formed at the Brill temperature in the copolyamide. Instead, crossing rather than merging of the (100) and the combined (010)−(110) WAXD reflections occurs upon heating of the copolyamides containing *trans*-1,4-DACH. In contrast to the cis isomer, introduction of *trans*-1,4-DACH into polyamide 4.14 raises the melting temperature, confirming the findings by solid-state NMR and WAXD analysis. Unlike 1,4-CHDA moieties, 1,4-DACH residues do not undergo thermal isomerization. Therefore, at the same amount of *initially* trans isomers, the copolyamides 4.14/1,4-DACH.14 exhibit higher second heating end melting points than the corresponding isomeric copolyamides 12.6/12.1,4-1,4-CHDA.

## 1. Introduction

The incorporation of cycloaliphatic monomers into polyesters and polyamides and the effects on the crystal structure and physical properties have been reported extensively.[1−15] Ridgway described isomorphism in polyamides of the type x.6 after incorporating 1,4-cyclohexanedicarboxylic acid (1,4-CHDA).[10] Kricheldorf and Schwarz described how incorporated 1,4-CHDA residues preferentially reside in the crystallites when they adopt a trans configuration.[2] We recently discussed the partial substitution of the linear aliphatic residues in the backbones of polyamides 12.6 and 4.14 by 1,4-CHDA and 1,4-diaminocyclohexane (1,4-DACH), respectively.[1,12−15] Relying on DSC measurements, wide-angle X-ray diffraction (WAXD), and solid-state NMR analysis, we concluded that *trans*-1,4-CHDA, as a result of its more stretched configuration, can be incorporated into the crystals of polyamide 12.6. In contrast, *cis*-1,4-CHDA causes kinks in the polymer chains and is therefore not tolerated in the crystalline phase of polyamide 12.6. Hence, *cis*-1,4-CHDA resides in the amorphous regions only. Preliminary thermal analysis pointed to a similar behavior when 1,4-DACH is introduced into the backbone of polyamide 4.14 (Figure 1). In contrast to cis cycloaliphatic residues, the incorporation of *trans*-1,4-DACH residues raises the melting point of the copolyamides compared to the homopolyamide 4.14.[14,15] Accordingly, a cocrystallization of the stretched trans cycloaliphatic residues and linear aliphatic residues is plausible. In the present article, we will provide evidence for this cocrystallization using solid-state NMR analysis and wide-angle X-ray characterization.

## 2. Experimental Section

**Molecular Characteristics and Crystallization of the Copolyamides.** We synthesized a series of copolyamides 4.14/1,4-DACH.14 from 1,12-dodecanedicarbonyl dichloride and a variable content of 1,4-diaminobutane (1,4-DAB) and 1,4-diaminocyclohexane (1,4-DACH) residues (see Figure 1), the latter having a variety of cis/trans ratios. The polycondensation reactions involved are described elsewhere together with details on how $^{1}$H-decoupled solution $^{13}$C NMR was used to determine the copolyamide composition and the cis/trans ratio of the cycloaliphatic residues in the polymer main chain.[13] The latter paper also provides information on the procedures adopted in the determination of the copolyamide intrinsic viscosities and molecular weight by SEC. The sample characteristics are listed in Table 1 together with their DSC melting points to be discussed below.

All solid (semicrystalline) structures of the polyamides, analyzed in this paper by WAXD and NMR, were obtained

[†] Free University of Brussels.
[‡] Catholic University of Leuven.
[§] Eindhoven University of Technology.
[⊥] DUBBLE-CRG/ESRF.
[#] Eindhoven University of Technology.
* To whom all correspondence should be addressed: e-mail c.e.koning@tue.nl.

10.1021/ma0500685 CCC: $30.25 
Published on Web 06/14/2005

**Table 1. Overview of Molecular Characterization and DSC End Melting Points of the Copolyamides 4.14/1,4-DACH.14**

| entry | molar ratio in final copolyamide 1,4-DAB/1,4-DACH[a] | molar ratio in final copolyamide cis/trans[a] | $[\eta]$ (dL g$^{-1}$) | $M_w$ (g mol$^{-1}$) | DSC end melting temp during second heating (°C) |
|---|---|---|---|---|---|
| R1 | 100/0 | | 0.53 | 50 000 | 228 |
| R2 | 93/7 | 0/100 | 0.59 | | 244 |
| R3 | 86/14 | 0/100 | 0.57 | 58 000 | 255 |
| R4 | 80/20 | 0/100 | 0.57 | 44 000 | 270 |
| R5 | 79/21 | 57/43 | 0.48 | | 239 |
| R6 | 80/20 | 75/25 | 0.44 | 38 000 | 227 |

[a] Determined by solution $^{13}$C NMR spectroscopy (experimental error: ca. 3%). These values slightly differ from the feed ratios as discussed in ref 13.

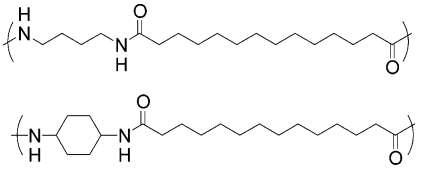

**Figure 1.** Chemical structure of repeating units of copolyamides 4.14/1,4-DACH.14.

directly after synthesis by precipitation from solution into a cold nonsolvent and subsequent drying under vacuum at 80 °C.

**Morphological and Thermal Characterization of the Copolyamides.** Details on the experimental procedures involved in the characterization of the thermal behavior (during first and second heating at 10 °C/min) by DSC and in the room temperature and high temperature crystal structure evaluation by time-resolved (synchrotron) WAXD can be found in earlier work.[1] The thermal program involved in the DSC characterization of all samples involves heating from 30 to 300 °C, 30 min isothermal annealing at 300 °C, cooling to 30 °C, and finally a second heating after 5 min again to 300 °C. The time-resolved WAXD measurements were performed at the DUBBLE CRG (Dutch-Belgian beamline) at the ESRF in Grenoble, France. Here samples were heated at 10 °C/min, and scattering patterns were collected in consecutive time frames of 6 s, resulting in one pattern per °C.

Proton-decoupled solid-state $^{13}$C and $^{15}$N NMR spectra were recorded on a Bruker DMX500 spectrometer operating at a $^{1}$H, $^{13}$C, and $^{15}$N NMR frequency of 500, 125, and 50 MHz, respectively. A 4 mm magic-angle-spinning (MAS) probehead with a sample-rotation rate of 12.5 kHz was used for $^{13}$C NMR. $^{15}$N NMR spectra were recorded at a MAS rate of 4 kHz on a 7 mm MAS probehead. The radio-frequency power was adjusted to obtain a 5 $\mu$s 90° pulse for all three nuclei ($^{1}$H, $^{13}$C, and $^{15}$N). The 38.56 ppm resonance of adamantane was used for external calibration of the $^{13}$C chemical shift and the 32 ppm signal of crystalline glycine for $^{15}$N NMR. To enhance the $^{13}$C and $^{15}$N NMR signal, cross-polarization (CP) was carried out with a contact pulse of 1 ms. The $^{13}$C and $^{15}$N pulse had the standard rectangular shape, whereas the amplitude of the proton pulse was linearly ramped. Proton spin−lattice relaxation times in the laboratory and rotating frame, $T_1\{^1H\}$ and $T_{1\rho}\{^1H\}$, were measured for each of the polymer components separately via CP to the $^{13}$C nuclei. Proton $T_{1\rho}$-filtered $^{13}$C NMR spectra were recorded with a filter time (duration of the proton lock pulse prior to the simultaneous CP pulses on both channels) of 1 and 20 ms and, respectively, using ca. 2000 and 10 000 scans. Line shape decomposition was carried out with the Bruker program WinFit with a set of nine Gaussian components with fixed positions and line widths and the heights as free fitting parameters. The procedure to select the positions and line widths is described in the discussion.

## 3. Results and Discussion

**Thermal Properties.** Figure 2 displays the first and second heating runs for three representative samples (R1, R4, and R5). The first heating runs (full lines) reflect the melting behavior of the synthesized samples and are relevant for comparison with the (time-resolved)

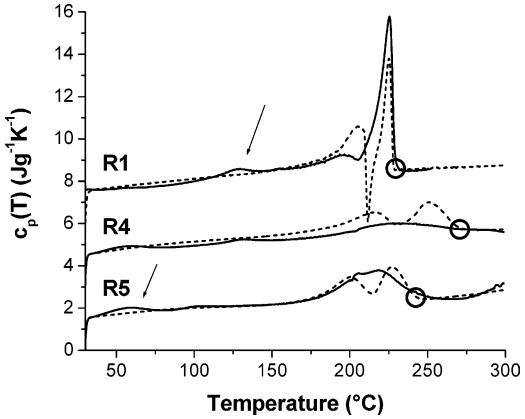


**Figure 2.** DSC first (full line) and second (dashed line) heating curves for (R1) polyamide 4.14, (R4) 20 mol % 1,4-DACH (cis/trans: 0/100), and (R5) 21 mol % 1,4-DACH (cis/trans: 57/43). The arrows highlight the endothermic "annealing peaks" related to the drying stage at 80 °C (peak in first heating runs at about 120 °C) and due to storage at room temperature (peak in first heating runs at about 50 °C). The circles indicate the end of melting. The curves for R1 and R4 are shifted 6 and 3 J g$^{-1}$ K$^{-1}$, respectively, for clarity.

WAXD and NMR results. The endothermic maxima highlighted with arrows at about 50 and 125 °C are due to isothermal annealing at room temperature and drying at 80 °C, respectively. Obviously, these maxima do not appear in a second heating run (dashed lines). Melting of the sample crystallites during first heating occurs over a quite broad temperature range. The onset for all samples is similar and occurs close to 170 °C. The shapes of the melting peaks differ from sample to sample and so do the end melting temperatures. The latter are highlighted with open circles. The copolymers all display single melting peaks during first heating whereas the homopolymer, R1, exhibits a small shoulder at the low temperature side of the main melting peak, which is due to partial melting and recrystallization as experiments at different heating rates indicated (not shown). This melting and recrystallization is inflated during second heating and also appears in the copolymers, indicating that the crystals obtained directly after synthesis are more stable compared to crystals that are grown from the melt during cooling. The melting onsets and end melting temperatures, however, are identical to the values associated with the first heating run. For sample to sample comparison we considered the end melting temperature obtained from the second heating run since due to a poor thermal contact between the (fluffy) sample and pan in the first heating run, some curvature can be observed in a number of experiments that hamper an accurate reading of the end melting temperature. Furthermore, we refrained from using the first heating peak melting temperature since the peaks are very broad and accordingly so are the distributions

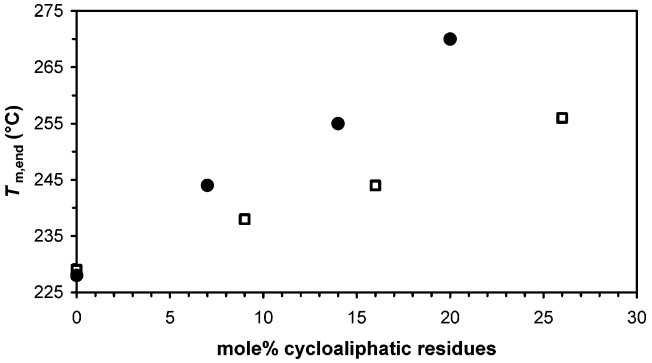


**Figure 3.** Second heating melting points of the copolyamides as a function of composition. Legend: (●) copolyamides 4.14/*trans*-1,4-DACH.14; (□) copolyamides 12.6/12.*trans*-1,4-CHDA.

of the crystal stability. By using the end melting temperature, the most stable crystals are considered selectively in this comparison. All values are collected in Table 1.

The end melting points, as obtained from the second heating DSC curves of the copolyamides 4.14/1,4-DACH.14, containing no cycloaliphatic diamine or only the trans isomer of 1,4-DACH, are shown in Figure 3 (●). For comparison, the second heating end melting points of the isomeric copolyamides 12.6/12.1,4-CHDA, synthesized with initially pure *trans*-1,4-CHDA, and taken from ref 1, are added to the same figure (□). As expected from their equal amide bond densities in their backbones, we find almost identical melting points for the linearly aliphatic isomers polyamide 12.6 and polyamide 4.14. Similar to the copolyamides 12.6/12.1,4-CHDA, the incorporation of the "stretched" trans cycloaliphatic (*trans*-1,4-DACH) residues into the backbone of polyamide 4.14 leads to an increased melting point for the copolyamides in comparison to the homopolyamide. In the former case the increased melting temperature was found to be associated with the ability of *trans*-1,4-CHDA residues to accommodate in a common crystal lattice with polyamide 12.6 segments. Whether or not also 1,4-diaminobutane (1,4-DAB) residues and *trans*-1,4-DACH residues fit into the same crystals is the focus of the remaining part of this paper. The melting point data in Table 1 furthermore show that 1,4-DACH residues that are predominantly cis do not give rise to an increase of the melting temperature. Using WAXD and solid-state NMR analysis, we have previously shown that cis moieties are not tolerated in the crystalline phase of the copolyamides 12.6/12.1,4-CHDA.[1] However, there is an important difference between the copolyamides 4.14/1,4-DACH.14 and 12.6/12.1,4-CHDA, as discussed next.

Compared to the isomeric copolyamides 12.6/12.1,4-CHDA, containing the same amounts of initially *trans*-1,4-CHDA, copolyamides 4.14 with incorporated *trans*-1,4-DACH show a higher second heating $T_m$. In the case of substitution of 14 mol % 1,4-DAB with all *trans*-1,4-DACH in polyamide 4.14 (entry R3), a rise in second heating $T_m$ of 27 °C is achieved. However, substituting 16 mol % of adipic acid with *trans*-1,4-CHDA in polyamide 12.6 results in an increase in the second heating $T_m$ of only 15 °C. The explanation for this difference can be found in the isomerization of the 1,4-CHDA residues: after the thermal treatment, taking place after the first heating run in the DSC, part of the *trans*-1,4-CHDA residues has been converted into *cis*-1,4-CHDA residues. In this way, the content of *trans*-1,4-CHDA in the copolyamide 12.6/12.1,4-CHDA has become lower than the initial content. Accordingly, after partial isomerization of trans into cis moieties during the first melting, less cycloaliphatic residues are available for incorporation into the crystals, resulting in lower melting and crystallization temperatures in the cooling and second heating DSC curves, respectively. The stability of 1,4-DACH-based polyamides was proven by solution $^{13}C$ NMR analysis of a copolyamide 4.14/1,4-DACH.14 as synthesized and after submission to 300 °C for 30 min.[13] The cis/trans ratio of this copolyamide did not change (within experimental error) during this thermal treatment. Hence, the total content of trans cycloaliphatic residues in the copolyamides 4.14/1,4-DACH.14 (and accordingly the content of cycloaliphatic residues in the crystals) is higher compared to copolyamides 12.6/12.1,4-CHDA, resulting in a higher melting point for the 1,4-DACH-based isomers.

In the case of copolyamides 12.6/12.1,4-CHDA, the second heating melting point of the copolyamides is independent of the initial cis/trans ratio of the 1,4-CHDA residues, provided that the residence time in the melt was sufficiently long to reach the cis/trans equilibrium (which was the case after 30 min at 300 °C).[1] In the case of the copolyamides 4.14/1,4-DACH.14, the initial cis/trans ratio of the cycloaliphatic residues has a large influence on the melting point determined from the second heating curve. For a copolyamide 4.14/1,4-DACH.14 containing 20 mol % all *trans*-1,4-DACH (entry R4) a second heating melting point of 270 °C is found. Incorporating a comparable amount of 1,4-DACH (21 mol %) having a cis/trans ratio of 57/43 (entry R5) results in a melting point of only 239 °C. For a copolyamide 4.14/1,4-DACH.14 containing 20 mol % 1,4-DACH with an even higher cis/trans ratio (75/25) (entry R6) a melting point of 227 °C is retrieved, which is similar to the melting point obtained for PA 4.14 (228 °C). These results strongly indicate that the cis cycloaliphatic DACH residues are not incorporated into the crystalline phase. This paper is devoted to collecting reliable WAXD and solid-state NMR evidence on the suggested cocrystallization in the 1,4-DACH-based copolyamides.

**Room Temperature WAXD Analysis.** In general, the WAXD pattern of semicrystalline polymers is composed of distinctive, more-or-less sharp diffraction signals originating from the crystalline phase, superimposed on a broad halo from the amorphous phase. Most polyamides give rise to two characteristic diffraction signals, at spacings around 0.44 and 0.37 nm. The former diffraction signal (indexed 100) yields information about the interchain distance within a hydrogen-bonded sheet, whereas the latter (a superposition of 010 and 110 reflections) is a measure for the distance between the separate sheets.[16] Consequently, using Bragg's law, we can interpret the WAXD data obtained for the copolyamides 4.14/1,4-DACH.14 in terms of interchain and intersheet distances.

As for the copolyamides 12.6/12.1,4-CHDA studied before,[1] we performed room temperature WAXD measurements on the copolyamides 4.14/1,4-DACH.14, for which the crystalline phase was formed during precipitation from solution (see Figure 4). The diffraction pattern of polyamide 4.14 (curve R1) clearly shows the two typical reflections, representing the interchain ($d$ = 0.442 nm, around $2\theta = 20°$) and intersheet distances

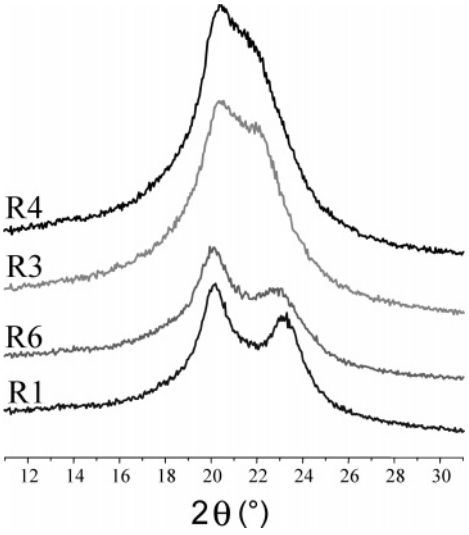


**Figure 4.** Room temperature WAXD analysis of "as synthesized" copolyamides 4.14/1,4-DACH.14 as a function of composition ($\lambda = 1.542$ Å). Legend: (R1) polyamide 4.14; (R6) 20 mol % 1,4-DACH (cis/trans: 75/25); (R3) 14 mol % 1,4-DACH (cis/trans: 0/100); (R4) 20 mol % 1,4-DACH (cis/trans: 0/100). The curves were shifted along the *y*-axis for clarity.

($d = 0.386$ nm, around $2\theta = 23°$). Comparison of these values with the data found for polyamide 12.6[1] shows a comparable interchain distance for both polyamides, but a slightly denser packing of the crystalline structure of polyamide 12.6 (smaller intersheet distance; $d = 0.377$ nm), without resulting into a significant difference in melting point as already mentioned. The partial substitution in polyamide 4.14 of 1,4-diaminobutane with 1,4-DACH, having a high cis isomer content, results in a copolyamide with a diffraction pattern (curve R6) similar to the one found for polyamide 4.14 (curve R1). This result is in line with the results obtained for the copolyamides 12.6/12.1,4-CHDA;[1] since cis moieties are excluded from the crystalline regions, their introduction into the polymer chain will have little effect on the crystalline structure of the copolyamides. In agreement with the copolyamides 12.6/12.1,4-CHDA, incorporation into the polyamide 4.14 main chain of 1,4-DACH moieties with a high content of trans isomers yields copolyamides that obtain a crystalline structure upon precipitation from solution (curve R3 and R4) differing from that of polyamide 4.14 (curve R1). The incorporation of trans cycloaliphatic residues in polyamide 4.14 results in a clear shift in the intersheet distance (from 0.386 to 0.407 nm), whereas the interchain distance remains more or less constant (minor shift from 0.442 to 0.436 nm). These results prove the possibility of the incorporation of trans cycloaliphatic residues into the crystalline phase of the copolyamides 4.14/1,4-DACH.14, for which preliminary indications were already obtained by thermal analysis. In agreement with the *trans*-1,4-CHDA residues incorporated in the crystalline phase of copolyamides 12.6/12.1,4-CHDA, the invariance of the interchain distance and the increase of the intersheet distance upon substitution of 1,4-diaminobutane with *trans*-1,4-DACH indicate the perpendicular orientation of the cyclic residues with respect to the plain of the hydrogen-bonded polymer chains.

Interestingly, we have recently found that cycloaliphatic piperazine.14-based repeating units, incorporated into the main chain of linearly aliphatic polyamide 2.14, are able to cocrystallize into a common crystal lattice with the 2.14 repeating units, but in this case the cycloaliphatic rings proved to be oriented parallel to the hydrogen-bonded sheets.[17]

**Temperature-Dependent WAXD Analysis.** It is known that when aliphatic polyamide crystals are heated, the two characteristic diffraction signals shifts toward one another and merge at the Brill temperature ($T_B$) to a Brill spacing of ca. 0.42 nm.[18] This single diffraction signal remains until melting ($T_m$), and the corresponding spacing only increases slightly as a consequence of thermal expansion. The high-temperature crystalline phase between $T_B$ and $T_m$, for which the interchain and the intersheet distances have become equal, is often referred to as pseudohexagonal.[16,18−26] Some polyamides have Brill temperatures lower than their $T_m$ (e.g., polyamides 6.6,[16,20] 4.6,[23] 6.8,[23] 4.4, 6.4, 8.4, 10.4, and 12.4[24]), whereas for others the $T_B$ and $T_m$ are coincident (e.g., 4.8, 4.10, 4.12, 6.10, 6.12, 6.18, and 8.12[19]). Upon heating the polyamides, the alkane segments within the nylon chains become increasingly mobile. They undergo restricted rotations, or liberations, and the intersheet 0.37 nm spacing increases, indicative of the increased alkane segment motion in this direction. On the other hand, because of their connecting hydrogen bonds, the amide groups are more constrained. At the Brill transition, the alkane segments have attained the same mobility in the intersheet direction, as they possess within the sheets. This had led some authors to propose that the Brill transition merely represents the attainment of a "rotator" phase for the alkane segments but that the hydrogen bonds remain intact in the original sheets.[27−29] However, according to Jones et al.,[19] this increased torsional flexibility of the alkane segments exerts a torsional force on the more rigid amide groups, a proportion of which then flips out (by ca. 60° or even ca. 120°) to form intersheet hydrogen bonds. These intersheet hydrogen bonds pin the nylon chains onto the pseudohexagonal lattice sites and prevent the chains from moving further apart. Irrespective of whether or not the rotator phase contains intersheet hydrogen bonds, it certainly is more disordered than the α-phase and, as a result, is favored at higher temperatures.

The transformation of the crystalline structure as a function of the temperature will most likely depend on the comonomer composition and stereochemistry of the copolyamides discussed in this paper. In particular, changes are expected for the polymers with incorporated *trans*-1,4-DACH residues, given the increased intersheet distance. Figure 5 shows the change in the crystalline structure upon heating of "as synthesized" copolyamides 4.14/1,4-DACH.14 with variable comonomer contents and cis/trans ratios, as studied by temperature-dependent WAXD analysis. The intensity of the scattering is represented with a gray scaling. As expected, polyamide 4.14 (Figure 5, R1) shows a behavior similar to its isomer polyamide 12.6.[1] The two diffraction signals shift toward each other and merge at the Brill temperature (ca. 160 °C), resulting in the pseudohexagonal phase. A similar Brill temperature was found for polyamide 12.6 ($T_B$ = ca. 160 °C). As for the copolyamides 12.6/12.1,4-CHDA,[1] the transformations of copolyamides 4.14/1,4-DACH.14 containing cycloaliphatic residues with a high cis/trans ratio (see Figure 5, R6) resemble those of the homopolyamide, in this case polyamide 4.14. This could be expected in view of the exclusion of cis moieties from the crystals. For the *trans*-1,4-DACH-based copoly-

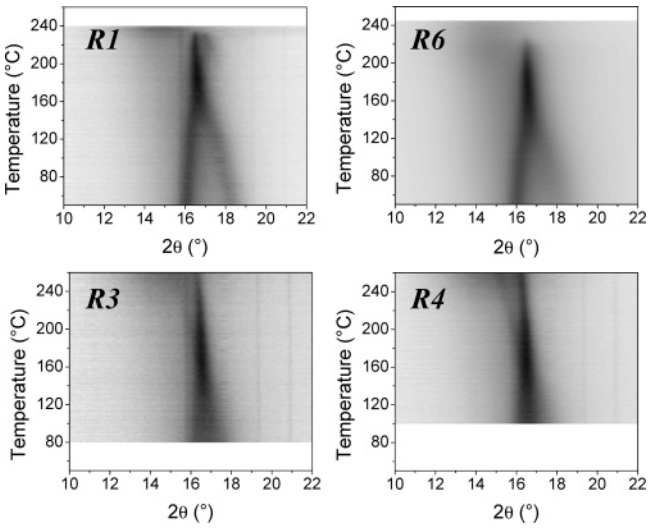


**Figure 5.** Temperature-dependent WAXD analysis of the first heating of copolyamides 4.14/1,4-DACH.14 as a function of composition ($\lambda = 1.218$ Å). Legend: (R1) polyamide 4.14; (R6) 20 mol % 1,4-DACH (cis/trans: 75/25); (R3) 14 mol % 1,4-DACH (cis/trans: 0/100); (R4) 20 mol % 1,4-DACH (cis/trans: 0/100). The starting temperature of all samples was adjusted to give all samples the same exposure time. The actual temperature window of a given sample depends on the expected final melting of the copolyamide.

amides, the variation of the diffraction pattern with temperature shows a crossing of the two reflections rather than a merging (see Figure 5, R3 and R4). However, this crossing is less well visible (and clearly dependent on the 1,4-DACH content) compared to the similar crossing observed and reported earlier for copolyamides 12.6/12.*trans*-1,4-CHDA.[1] Since at room temperature the difference in intersheet and interchain distances is less pronounced for the copolyamides 4.14/1,4-DACH.14 based on pure *trans*-1,4-DACH in comparison to the copolyamides 12.6/12.1,4-CHDA, their shift as a function of temperature is less pronounced as well. Furthermore, this crossing in the case of the copolyamides 4.14/1,4-DACH.14 is clearly dependent on the 1,4-DACH content. In agreement with the *trans*-1,4-CHDA-based copolyamides, the "as synthesized" copolyamides 4.14/1,4-DACH.14 containing *trans*-1,4-DACH residues do not melt from the pseudohexagonal phase, which is usually reported as being typical for even−even polyamides.[16,19]

As for the copolyamides 12.6/12.1,4-CHDA, the reduction of the rotational mobility of the amide bonds connected to cyclic aliphatic residues in comparison to the linear aliphatic residues may explain this crossing: the formation of intersheet hydrogen bonds, involving the breaking of the some of the regular interchain hydrogen bonds and flipping of amide bonds out of the hydrogen-bonded sheets, may be prevented. Another possible explanation may be found in the lowering of the symmetry needed for attainment of the pseudohexagonal phase by the introduction of the *trans*-1,4-DACH residues in the crystalline phase.

**Solid-State NMR Analysis.** In a previous study we used solid-state NMR experiments to investigate the partial substitution of the linear adipic acid in polyamide 12.6 by 1,4-CHDA.[1] Similarly to, e.g., semicrystalline polyethylene,[30] a splitting of the aliphatic signals was observed in the magic-angle-spinning (MAS) $^{13}$C NMR spectrum, with two major signals at 34 and 31 ppm respectively assigned to the $CH_2$ moieties in the crystalline and amorphous phase. Proton $T_{1\rho}$ and $T_1$ relaxation measured through each of the two $^{13}$C NMR signals indicated domain sizes between 1 and 50 nm, in rough agreement with the typical lamellar thickness of polyamides of about 5 nm.[16] In addition, the $^{13}$CO signals of the adipic acid and the 1,4-CHDA components in the polyamide were well-resolved in the MAS $^{13}$C NMR spectrum (Figure 6). Combined with proton relaxation measurements, we could exploit this to determine the distribution of trans and cis isomers of 1,4-CHDA over the crystalline and amorphous phase. *trans*-1,4-CHDA turned out to be equally distributed, like the adipic moieties, over the two phases, whereas *cis*-1,4-CHDA was located in the amorphous phase, as expected from stereochemistry and in full agreement with DSC and WAXD results.

In the present study we have initially applied the same strategy to determine the location of 1,4-diaminocyclohexane (1,4-DACH) as a comonomer in polyamide 4.14. However, no splitting of the amide signal is visible in the cross-polarization (CP) MAS $^{13}$C NMR spectrum (Figure 6). In contrast to the previous CHDA case of which the amide signals are also shown in Figure 6, none of the $^{13}$C nuclei in the amide bonds in DACH-containing copolyamides are directly vicinal to the tertiary carbons of the cycloaliphatic residue. In the primary sequence there is at least one nitrogen in between. Expecting that the difference between the cyclic and linear diamine residue may be felt more strongly by nitrogen atoms, we have searched for a splitting of the amide signal in the CPMAS $^{15}$N NMR spectrum as well. $^{15}$N is a relatively insensitive NMR isotope, and large numbers of scans are required for spectra from natural-abundance samples. A similar, 10 ppm broad signal at ~116 ppm, i.e., ca. 80 ppm upfield with respect to crystalline glycine,[31,32] is observed for both the homo- and copolyamide. Compared to the homopolyamide 14.4, no further line broadening or splitting is found for the copolyamide with 20% 1,4-DACH. Careful reinspection of the aliphatic region in the $^{13}$C NMR spectra with and without 1,4-DACH, however, reveals a new signal at ~48 ppm for the copolymer containing 20% 1,4-DACH completely in the trans form. We tentatively assign this signal to CH next to NH in 1,4-DACH. Indeed, a rough estimation of the $^{13}$C NMR shift based on linear substituent effects predicts this resonance to be ca. 2 ppm downfield from the C1 in linear 1,4-diaminobutane. At the same position, there appears to be a small, but significant, and reproducible shoulder in the spectrum of the copolymer containing 20% 1,4-DACH mainly in the cis form (75% cis, 25% trans). Despite the similar overall 1,4-DACH content of 20%, this signal is lower than for the *trans*-1,4-DACH containing copolymer. Since $^1$H−$^{13}$C cross-polarization is more effective for rigid than for mobile polymers, *cis*-1,4-DACH appears to be located in a more mobile polymer environment than *trans*-1,4-DACH.

The resolved $^{13}$C resonance of 1,4-DACH at ~48 ppm offers the opportunity to selectively study the NMR relaxation properties of the protons in 1,4-DACH and their local vicinity in the copolymer, and, in this way, allows determining the distribution of 1,4-DACH over the crystalline and amorphous phase. As a result of spin diffusion, protons in a solid polymer tend to show spatially averaged spin−lattice relaxation properties over $10^{-9}$−$10^{-6}$ m, depending on the relaxation time scale and the effective dipole interactions between the

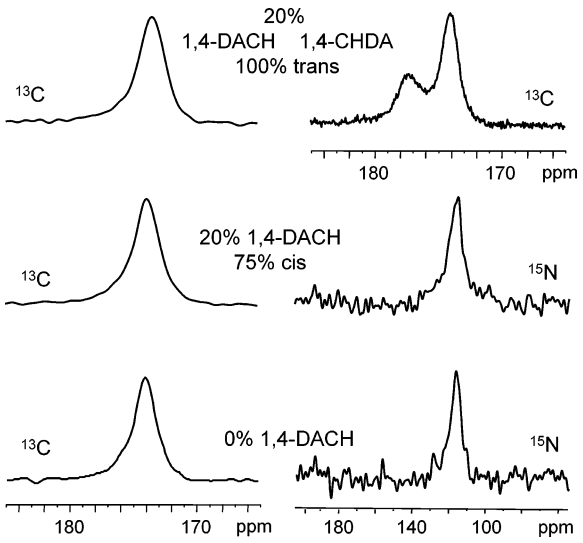


**Figure 6.** Amide region in the CPMAS $^{13}$C (left) and $^{15}$N (right) NMR spectra of (lower) the polyamide PA 4.14 (1K scans); (middle) a copolyamide 4.14/1,4-DACH.14 containing 20 mol % 1,4-DACH (75/25 cis/trans) (4K scans). The top figures represent the $^{13}$C NMR spectra of a copolyamide (left) with 20% *trans*-1,4-DACH and (right) with 20% *trans*-1,4-CHDA for comparison.

protons. Standard $^1$H $T_{1\rho}$ relaxation measurements suggest that the aliphatic line shape between 50 and 20 ppm contains different components, with a maximum $T_{1\rho}$ value of ca. 10 ms found at 33 ppm. However, the 1,4-DACH signal at 48 ppm is too small to accurately determine relaxation rates, like we did in our previous study. Instead, we have focused on recording two $T_{1\rho}$ relaxation filtered spectra with respective filter times of 1 and 20 ms at the highest achievable signal-to-noise ratio for all three examined samples (Figure 7).

To compare the various $T_{1\rho}$ filtered spectra and identify fast and slowly relaxing components, we decomposed the six resulting spectra in terms of a given set of nine Gaussian components with fixed positions and line widths and variable amplitudes (Table 2). Figure 7 shows the resulting decomposition of the aliphatic region in the $^{13}$C NMR spectrum. The positions and line widths of the lines at 21.5, 28.5, 33.4, 37.0, and 40.6 ppm were chosen on the basis of the 20 ms filtered spectrum of polyamide 4.14. At this relatively long filter time the spectrum is supposedly dominated by the crystalline phase. Two components, at 30.8 and 39.4 ppm, were added to explain the different line shape of the same material at a filter time of 1 ms and probably cover fast decaying signals from the amorphous phase. The eighth and ninth components at 48.0 and 49.0 ppm were added to explain the spectral changes for the copolyamides containing 1,4-DACH residues. It should be emphasized that the nine components primarily offer a convenient mathematical line shape description. There need not be a one-to-one correlation to the real components underlying the line shape; e.g., the weak Gaussian component at 21.5 ppm may just reflect the upfield wing of the 28.5 ppm line. Nevertheless, the component at 33.4 ppm, which is the least affected by the relaxation filter, typically represents long all-trans $CH_2$ chains in the crystalline phase, in particular the methylenes separated by more than two positions in the primary sequence from the nearest CO group in the C14-dicarboxylic moieties. The two components at 37.0 and 40.6 ppm show the same relaxation behavior as the 33.4 ppm component and probably contain the $^{13}$C NMR signals from $CH_2$ groups directly connected to the amide unit C(O)N(H). By analogy, the fast decaying components at 30.8 and 39.4 ppm reflect the corresponding $^{13}$C nuclei in the amorphous phase. The signal at 28.5 ppm, as well as its upfield wing at 21.5 ppm, shows intermediate relaxation behavior and probably contains the signals of $CH_2$ groups at $\beta$-carbon positions relative to the amide units, both within the amorphous and the crystalline phase. Interestingly, the two components at 48.0 and 49.0 ppm in the $T_{1\rho}$-filtered spectra of the copolymer containing *trans*-1,4-DACH are increased with respect to in the spectrum of the homopolyamide

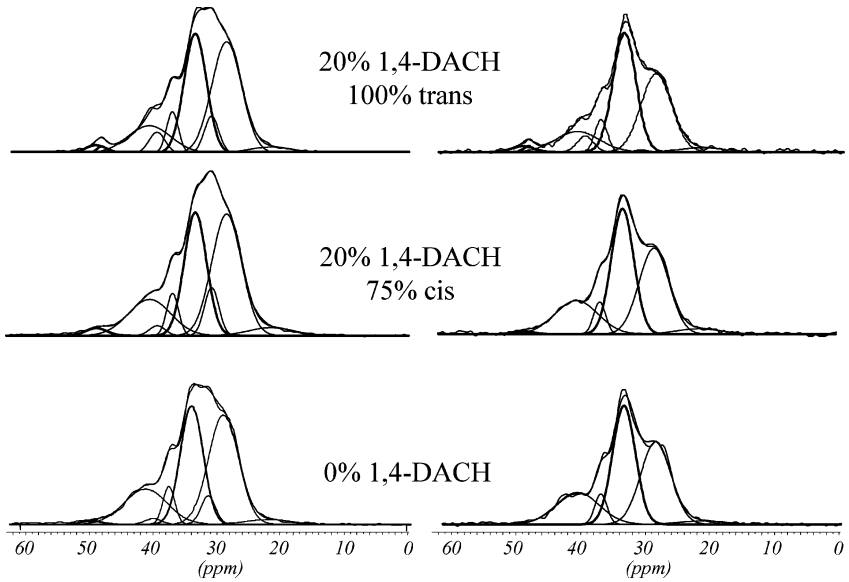


**Figure 7.** $T_{1\rho}$-filtered $^{13}$C NMR spectra at filter times of (left) 1 and (right) 20 ms of the same samples in the same top-down order as in Figure 6. All spectra have been decomposed in terms of a given set of nine Gaussian components with fixed positions and line widths and variable heights, yielding a model with essentially nine free fit parameters. The spectra are normalized with respect to the supposedly crystalline component at 33.4 ppm, which in reality has a $T_{1\rho}$ relaxation time of ca. 10 ms. For signal-to-noise improvement the 20 ms spectra were recorded with about five times more scans than the 1 ms (ca. 2000 and 10 000, respectively).

**Table 2. Line Shape Fit of Proton $T_{1\rho}$-Filtered MAS $^{13}C$ NMR Spectra of the Homopolyamide and the Copolyamide with DACH in the Trans or (Mainly) Cis Configuration[a]**

| | | | 0% DACH | | 20% DACH 100% trans | | 20% DACH 75% cis | | tentative assignt carbon type and phase |
|---|---|---|---|---|---|---|---|---|---|
| | $\sigma$ (ppm) | $\Delta\sigma$ (ppm) | I | R | I | R | I | R | |
| 1 | 49.0 | 4.0 | 0.03 | 0.15 | 0.06 | 0.37 | 0.06 | 0.07 | )*C*H−N(H): amorphous + foot of 40.6 ppm line |
| 2 | 48.0 | 1.8 | | | 0.02 | 0.28 | | | )*C*H−N(H): crystalline |
| 3 | 40.6 | 7.9 | 0.57 | 0.15 | 0.44 | 0.24 | 0.56 | 0.14 | −*C*$H_2$−N(H): both |
| 4 | 39.0 | 2.9 | 0.05 | 0.00 | 0.12 | 0.25 | 0.06 | 0.00 | −*C*$H_2$−C(O): amorphous |
| 5 | 37.0 | 2.2 | 0.17 | 0.14 | 0.18 | 0.25 | 0.18 | 0.12 | −*C*$H_2$−C(O): crystalline |
| 6 | 33.4 | 4.1 | 1 | 0.17 | 1 | 0.32 | 1 | 0.16 | −(*C*$H_2$)$_n$: crystalline |
| 7 | 30.8 | 2.7 | 0.25 | 0.01 | 0.20 | 0.02 | 0.25 | 0.00 | −($CH_2$)$_n$: amorphous |
| 8 | 28.5 | 5.5 | 1.23 | 0.12 | 1.24 | 0.23 | 1.31 | 0.11 | −*C*$H_2$−$CH_2$−N(H): both; −*C*$H_2$−; $CH_2$−C(O): both |
| 9 | 21.5 | 8.2 | 0.08 | 0.19 | 0.10 | 0.22 | 0.13 | 0.11 | foot of 28.5 ppm line |

[a] The aliphatic region of the spectra is decomposed in terms of nine Gaussian components with fixed chemical shift positions $\sigma$ and line widths $\Delta\sigma$, and variable amplitudes. Instead of amplitudes, we here report the integrals I in the spectra recorded at a filter time of 1 ms relative to the respective 33 ppm components. For every component separately, the amplitude decrease in the spectra at a filter time of 20 ms, relative to that at 1 ms, is indicated by a scaling ratio $R$.

(Table 2). The $T_{1\rho}$ scaling of these two components is in the order of 0.3, similar to the scaling of the 33.4 and 28.5 ppm signal. This indicates that a large fraction of *trans*-1,4-DACH is located in the crystalline phase. In contrast, the 1,4-DACH signal at 49.0 ppm for the predominantly *cis*-1,4-DACH containing copolymer shows faster relaxation than the 28.5 ppm signal, indicating that 1,4-DACH in this material is mainly located in the amorphous phase. Some residual intensity at this position in the spectra of the homopolyamide and the 20 ms filtered spectra of the copolyamide may arise from the downfield wing of the 40.6 ppm line assigned to the 1,4-DAB-based repeating units.

## 4. Conclusions

In agreement with the results earlier obtained for partially cycloaliphatic copolyamides 12.6/12.1,4-CHDA,[1] the configuration of the cycloaliphatic residues in the isomeric copolyamides 4.14/1,4-DACH.14 is the determining factor in the cocrystallization of linear and cyclic aliphatic residues. The "stretched" trans isomer-based repeating units readily cocrystallize with the 1,4-diaminobutane-based residues as a solid solution rather than as defects, thereby increasing the melting point and expanding the room temperature crystalline structure. Thermal analysis, solid-state NMR data, and WAXD experiments clearly show the repulsion of the *cis*-1,4-DACH moieties from the crystalline phase. As for the copolyamides 12.6/12.1,4-CHDA, the presence of trans cycloaliphatic residues in the crystalline phase of the copolyamides 4.14/1,4-DACH.14 reduces the mobility of the chains and prevents the formation of a pseudohexagonal phase during heating prior to melting. In other words, a Brill transition to the so-called pseudohexagonal phase does not occur, and crossing rather than merging of the WAXD crystalline reflections is observed.

**Acknowledgment.** The authors acknowledge Prof. Dr. Ir. B. Van Mele and Ir. S. Swier (both FYSC, Free University of Brussels; VUB) for their help in the thermal characterization. B. Vanhaecht is grateful to the Fund for Scientific Research−Flanders (Belgium) (F.W.O.) for financing his Ph.D. study. B. Goderis is a postdoctoral fellow of the Fund for Scientific Research−Flanders.

## References and Notes

(1) Vanhaecht, B.; Willem, R.; Biesemans, M.; Goderis, B.; Basiura, M.; Magusin, P. C. C. M.; Dolbnya, I.; Koning, C. E. *Macromolecules* **2004**, *37*, 421.
(2) Kricheldorf, H. R.; Schwarz, G. *Makromol. Chem.* **1987**, *188*, 1281.
(3) Tenkovtsev, A. V.; Rutman, A. B.; Bilibin, Yu, A. *Makromol. Chem.* **1992**, *193*, 687.
(4) Osman, M. A. *Macromolecules* **1986**, *19*, 1824.
(5) Kwolek, S. L.; Luise, R. R. *Macromolecules* **1986**, *19*, 1789.
(6) Reck, B.; Ringsdorf, H.; Gardner, K.; Starkweather, H., Jr. *Makromol. Chem.* **1989**, *190*, 2511.
(7) Srinivasan, R.; Prasad, A.; Marand, H.; McGrath, J. E. *Polym. Prepr. (Am. Chem. Soc., Div. Polym. Chem.)* **1991**, *32*, 174.
(8) Srinivasan, R.; McGrath, J. E. *Polym. Prepr. (Am. Chem. Soc., Div. Polym. Chem.)* **1992**, *33*, 503.
(9) Srinivasan, R.; Moy, T.; Saikumar, J.; McGrath, J. E. *Polym. Prepr. (Am. Chem. Soc., Div. Polym. Chem.)* **1992**, *33*, 225.
(10) Ridgway, J. S. *J. Polym. Sci., Part A1* **1970**, *8*, 3089.
(11) Kalmykova, V. D.; Bogdanov, M. N.; Okromchedlidze, N. P.; Zhmayeva, I. V.; Yefremov, Ya, V. *Polym. Sci. USSR* **1967**, *9*, 2539.
(12) Vanhaecht, B.; Teerenstra, M. N.; Suwier, D. R.; Willem, R.; Biesemans, M.; Koning, C. E. *J. Polym. Sci., Polym. Chem.* **2001**, *39*, 833.
(13) Vanhaecht, B.; Rimez, B.; Willem, R.; Biesemans, M.; Koning, C. E. *J. Polym. Sci., Polym. Chem.* **2002**, *40*, 1962.
(14) Koning, C.; Vanhaecht, B.; Willem, R.; Biesemans, M.; Goderis, B.; Rimez, B. *Macromol. Symp.* **2003**, *199*, 431.
(15) Koning, C.; Vanhaecht, B.; Willem, R.; Biesemans, M.; Goderis, B.; Rimez, B. *Polym. Prepr. (Am. Chem. Soc., Div. Polym. Chem.)* **2003**, *44*, 1063.
(16) Jones, N. A.; Cooper, S. J.; Atkins, E. D. T.; Hill, M. J.; Franco, L. *J. Polym. Sci., Polym. Phys. Ed.* **1997**, *35*, 675.
(17) Hoffmann, S.; Vanhaecht, B.; Devroede, J.; Bras, W.; Rastogi, S.; Koning, C. E. *Macromolecules*, in press.
(18) Brill, R. *Z. Phys. Chem. (Munich)* **1943**, *61*, 1353.
(19) Jones, N. A.; Atkins, E. D. T.; Hill, M. J.; Cooper, S. J.; Franco, L. *Polymer* **1997**, *38*, 2689.
(20) Starkweather, H. W.; Whitney, J. F.; Johnson, D. R. *J. Polym. Sci., Polym. Phys. Ed.* **1963**, *1*, 715.
(21) Sandeman, I.; Keller, A. *J. Polym. Sci.* **1956**, *19*, 401.
(22) Ramesh, C.; Keller, A.;. Eltink, S. J. E. A. *Polymer* **1994**, *35*, 2483.
(23) Hill, M. J.; Atkins, E. D. T. *Macromolecules* **1995**, *28*, 604.
(24) Jones, N. A.; Atkins, E. D. T.; Hill, M. J.; Cooper, S. J.; Franco, L. *Macromolecules* **1996**, *29*, 6011.
(25) Jones, N. A.; Atkins, E. D. T.; Hill, M. J.; Cooper, S. J.; Franco, L. *Macromolecules* **1997**, *30*, 3569.
(26) Atkins, E. D. T.; Hill, M. J.; Jones, N. A.; Cooper, S J. *J. Polym. Sci., Polym. Phys. Ed.* **1998**, *36*, 2401.
(27) Flory, P. J.; Williams, A. D. *J. Polym. Sci., Part A2* **1967**, *5*, 399.
(28) Hirschinger, J.; Miura, H.; Gardner, K. H.; English, A. D. *Macromolecules* **1990**, *23*, 2153.

(29) Wendoloski, J. M.; Gardner, K. H.; Hirschinger, J.; Miura, H.; English, A. D. *Science* **1990**, *247*, 431.

(30) Schmidt-Rohr, K.; Spiess, H. W. *Multidimensional Solid-State NMR and Polymers*; Academic Press Limited: London, 1994; Chapter 7.

(31) Mathias, L. J.; Davis, R. D.; Jarrett, W. L. *Macromolecules* **1999**, *32*, 7958.

(32) Inês, M.; Tavares, B.; de Souza, C. M. G. *J. Appl. Polym. Sci.* **2003**, *90*, 3872.

MA0500685